

# Effect of Length of Hydroxyalkyl Groups in the Clay Modifier on the Properties of Thermoplastic Polyurethane/Clay Nanocomposites

Wantaek Kim,<sup>1</sup> Dae-won Chung,<sup>2</sup> Jeong Ho Kim<sup>1</sup>

<sup>1</sup>Department of Chemical Engineering, University of Suwon, Kyunggi-do, Korea

<sup>2</sup>Department of Polymer Science and Engineering, University of Suwon, Kyunggi-do, Korea

Received 27 September 2007; accepted 5 July 2008

DOI 10.1002/app.28929

Published online 8 September 2008 in Wiley InterScience (www.interscience.wiley.com).

**ABSTRACT:** Polyether- and polyester-based thermoplastic polyurethane (TPU) nanocomposites containing the montmorillonite modified with quaternary ammonium salts having a relatively long hydroxyalkyl branch (MMT-OH) were prepared via solution mixing. Quaternary ammonium salts with dimethyl, octyl, hydroxyundecyl branches were synthesized by the addition reaction of dimethyloctylamine and 11-bromo-1-undecanol and were used for the preparation of MMT-OH. In this MMT-OH clay, hydroxyl groups are located at the outer end of the relatively long undecyl branch, which may make the hydroxyl groups more exposed to the matrix polymers compared to the clays with the modifiers having shorter hydroxyalkyl chain such as C30B. Actually, more hydroxyl groups in MMT-OH's are thought to be exposed outside the modified clay, since MMT-OH's were observed to be somewhat dispersed in water, while clays with shorter alkyl chains were not. From XRD and TEM results, the silicate layers of MMT-OH were

shown to be very well dispersed in ether-TPU and ester-TPU nanocomposites prepared from dimethyl acetamide solution. In the case of ester-TPU nanocomposites, much better clay dispersion was observed for nanocomposites containing MMT-OH than the ones with C30B in the TEM images. The tensile properties measurement showed the similar trend. Although MMT-OH has only one hydroxyl group while C30B has two, above results of better tensile properties and water dispersibility of MMT-OH than C30B having two hydroxyls indicate that the position of hydroxyls may be an important factor in determining the properties of TPU/clay nanocomposites. Fourier transform infrared spectroscopy analyses showed that the long hydroxyalkyl chain modifiers may provide more hydrogen bonding sites than short hydroxyalkyl chain modifiers. © 2008 Wiley Periodicals, Inc. *J Appl Polym Sci* 110: 3209–3216, 2008

**Key words:** polyurethane; clay; nanocomposites

## INTRODUCTION

In recent years, great deal of studies on polymer/clay nanocomposites have been reported because of several advantages that can be achieved by the addition of clays such as improvement in heat stability and mechanical properties, and decreased gas permeability and flammability.<sup>1–6</sup> Since the first nanocomposite study on nylon 6/clay,<sup>7</sup> investigations on nanocomposites have been widely performed using a lot of polymers such as polyamide, epoxy, polystyrene, polyester, polypropylene, polyethylene, etc.<sup>8–15</sup> Nanocomposites of thermoplastic polyurethanes (TPUs) with nanoclays have also been studied since the first report by Wang and Pinnavaia.<sup>16</sup> TPU nanocomposites containing modified clays have been reported to show improved mechanical and thermal

properties compared to pure TPUs.<sup>17–24</sup> Since the compatibility between clays and polymers of interest forming nanocomposites are usually poor, clays such as montmorillonites are treated with organic salts. TPU nanocomposites with clay Cloisite C30B of Southern Clay Products (C30B) were reported to show a good dispersion of layered silicates because of the interaction between TPUs and hydroxyl functionalities of C30B.<sup>25–27</sup>

There is a report in the literature that the clay modifiers reside primarily in the interlayer, and not on the outer surface of clay even for the case that the clay is modified with an excess of the ion exchange capacity of natural clay, pristine montmorillonites (PM).<sup>26</sup> Although the possibility that some of the modifiers can still exist outside the surface of the clay cannot be excluded completely, most of the clay modifiers may exist inside the clay layers. Since clay C30B was treated with about the same modifier concentration (90 mequiv/100 g clay) as the ion exchange capacity of PM (92.6 mequiv/100 g clay) and does not possess excess modifier, only a small fraction of hydroxyl groups may exist at the outer

Correspondence to: J. H. Kim (jhkim@suwon.ac.kr).

Contract grant sponsor: Center for Environmental and Clean Technologies (designated by Ministry of Knowledge Economy in the University of Suwon).

surface of clays. One long alkyl chain (tallow) of C30B may even hinder the exposure of short hydroxyalkyl (two hydroxyethyls in C30B) chains to the matrix polymers. This may be supported by the observation that C30B is not dispersible in water even though C30B has two hydroxyl groups in the four branches of the modifier.

In this study, montmorillonite modified with quaternary ammonium salts having a relatively long hydroxyalkyl branch (MMT-OH) were prepared, where the hydroxyl groups are located at the very end of the undecyl chain to see the effect of length of alkyl chain in hydroxyalkyl group of the modifier. This relatively long undecyl chain may make the hydroxyl groups more exposed to the matrix polymers when the nanocomposites were prepared, compared to the clays treated with the hydroxyalkyl modifiers having shorter alkyl chain. Quaternary ammonium salts with only one hydroxyundecyl branch were synthesized to see whether even only one hydroxyl can cause some change in the clay dispersion of TPU/clay nanocomposites when the alkyl chains of hydroxyalkyl groups having hydroxyl groups at the end are made longer. Both polyester and polyether-based TPUs (ether-TPU and ester-TPU) were used to prepare nanocomposites with MMT-OH clay as well as with organically modified clays having two shorter hydroxyalkyl chains (C30B). Though direct comparison between MMT-OH nanocomposites and C30B ones cannot be made since MMT-OH has only one hydroxyl group while C30B has two, nanocomposites containing C30B may give some indication on the effect of position of hydroxyls on several properties compared to the ones containing MMT-OH clay.

TPU nanocomposites were prepared by solution mixing, and XRD and TEM analyses were performed to check the state of clay dispersion in the nanocomposites. The tensile properties were also measured, and the Fourier transform infrared spectroscopy (FTIR) analysis was carried out to investigate the interactions involved by the addition of aforementioned clays.

## EXPERIMENTAL

### Preparation of MMT-OH

Organic modifier, quaternary ammonium bromide with hydroxyl group (QAB-OH) at one chain end, was synthesized according to the general procedure of preparing quaternary ammonium salt from tertiary amine.<sup>28,29</sup> QAB-OH was synthesized by the addition reaction of dimethyloctylamine (DMOA) and 11-bromo-1-undecanol (BUDO) as shown in reaction scheme in Figure 1. DMOA (9.7 g, 62 mmol) and BUDO (13 g, 52 mmol) were dissolved in 10 mL

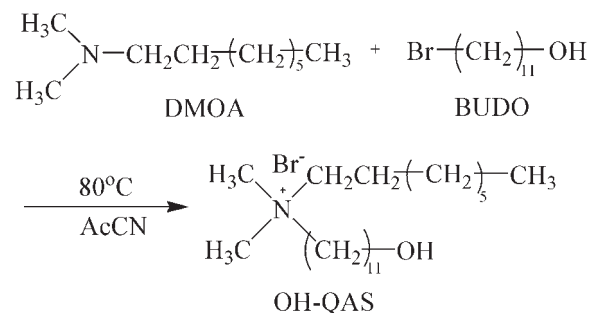


**Figure 1** Synthesis of quaternary ammonium bromide.

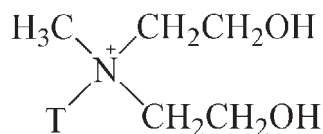
of acetonitrile and refluxed at 80°C. The progress of the reaction was monitored by TLC to observe the disappearance of a spot of unreacted BUDO. After 4 h, the reaction mixture was precipitated in 200 mL of diethyl ether, and kept at 4°C overnight. White precipitate was collected by filtration and dried under vacuum. QAB-OH (19.1 g), whose melting point is 106.8°C, was obtained with 91% yield.

MMT-OH was prepared by the ion exchange of PM with QAB-OH according to the reported method.<sup>30</sup> PM (10 g) was dispersed in 100 mL of methanol/water (1/9) at 40°C under continuous stirring to obtain the PM suspension. QAB-OH (7.2 g) predissolved in 50 mL of methanol/water (1/9) was poured into the PM suspension and stirred at 200 rpm for 20 h at 40°C. A white precipitate was collected by filtration and washed with 200 mL of methanol/water (1/9) several times until no bromide ion was detected in the filtrate by the addition of AgNO<sub>3</sub>. After drying under vacuum (100°C, 5 h), MMT-OH (11.7 g) was obtained, and ground to pass 100 mesh before use.

### Materials and preparation of nanocomposites

Two types of TPUs were obtained from SK chemicals; polyether-based TPU (Skythane R185A,  $M_w \sim 2,50,000$ ) and polyester-based TPU (Skythane S185A,  $M_w \sim 2,50,000$ ) having the similar Shore Hardness of 87A. Hard segments of both ether type and ester type TPUs are made of 4,4'-diphenylmethane diisocyanate and 1,4-butanediol, but soft segments are different such as poly(tetramethylene oxide) glycol ( $M_w \sim 1000$ ) for ether type and poly(butylene adipate) glycol ( $M_w \sim 1000$ ) for ester type.

The organically modified clay with two relatively short hydroxyalkyl chains, C30B, was obtained from Southern Clay Products. Cloisite 30B (C30B, CEC: 90 mequiv/100 g) is a montmorillonite modified with a quaternary ammonium salt having one methyl, two short hydroxyalkyl (—CH<sub>2</sub>CH<sub>2</sub>OH) and one tallow (T), which is a long alkyl chain (mixture of C<sub>14</sub>, C<sub>16</sub>, and C<sub>18</sub>) as shown below.



Nanocomposites of ether-TPU (or ester-TPU) with MMT-OH (or C30B) were prepared using dimethylacetamide (DMAc) solvent. A solution of 5 wt % clay in DMAc was sonicated before being added to the solution of TPU in DMAc followed by stirring for 24 h at room temperature. The mixture was then cast onto a glass plate, and the resulting films were dried at 50°C for 5 days followed by subsequent drying for 4 days under vacuum.

### Nanocomposites characterization

The change in gallery distance of silicate layers in the clay was determined on X-ray diffractometer (D-8 Advance) using Cu K $\alpha$  radiation at 40 kV, 35 mA. The samples were scanned at 2° min<sup>-1</sup>. The basal spacing of the clay,  $d_{001}$ , was calculated using the Bragg's law ( $\lambda = 2d \sin \theta$ ).

TEM images of nanocomposite specimens were obtained using Energy Filtering-Transmission Electron Microscopy (EM-912 OMEGA, Carl Zeiss Co.), with an operating voltage of 120 kV at the Korea Basic Science Institute. The ultrathin sectioning was performed on ultramicrotome at -100°C.

Tensile tests were carried out on a universal testing machine (LR10K LLOYD Instrument), according to ASTM D 882 method. The crosshead speed was 200 mm/min, and at least five measurements were taken.

FTIR was performed on FTIR-4200 (Jasco) at a resolution of 4 cm<sup>-1</sup>.

## RESULTS AND DISCUSSION

### MMT-OH preparation

Organic modifier, QAB-OH obtained as described in the Experimental section was characterized by <sup>1</sup>H NMR in CDCl<sub>3</sub>. <sup>1</sup>H NMR spectra were obtained by Spectrometer FT-NMR (500 MHz) of Bruker using CDCl<sub>3</sub> as a solvent. As shown in Figure 2, the chemical shifts and integration ratios of all signals are in good agreement with the expected values of QAB-OH. Absence of -CH<sub>2</sub>- adjacent to tertiary amine of unreacted DMOA, which appears in 2.6 ppm if remained, demonstrated the complete reaction.

MMT-OH was prepared by ion exchange of PM with QAB-OH. The organic content of modified MMT is generally calculated from the weight loss at 500°C.<sup>31</sup> TGA analysis of MMT-OH showed 21% weight loss at 500°C, whereas 19% was observed for C30B.

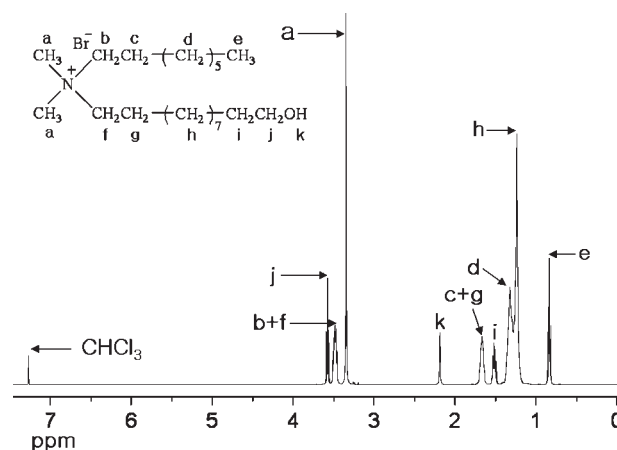
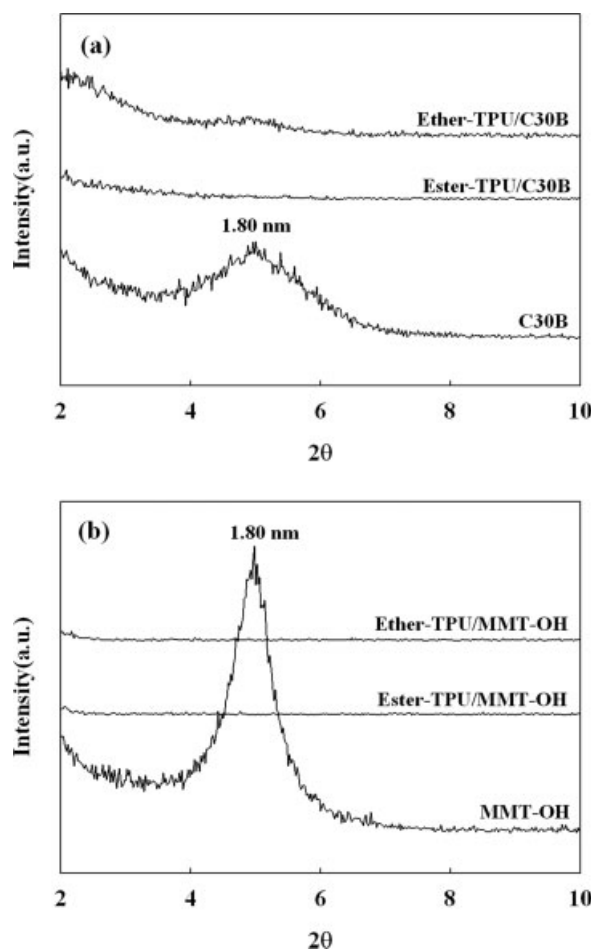


Figure 2 NMR data of quaternary ammonium bromide.

### Morphology

X-ray diffraction (XRD) results are obtained for nanocomposites with 5 wt % MMT-OH or C30B. Figure 3(a) shows XRD patterns for clay 30B itself and ether-TPU/C30B and ester-TPU/C30B nanocomposites prepared from DMAc solution. Clay C30B exhibits a peak at  $2\theta = 4.9^\circ$  ( $d$  spacing = 1.80 nm), while almost no peaks are observed for both ether-TPU and ester-TPU nanocomposites indicating a very good dispersion of clays in TPU matrices as reported in several previous studies.<sup>18,24-27</sup> Figure 3(b) shows XRD patterns for clay MMT-OH itself, and ether-TPU/MMT-OH and ester-TPU/MMT-OH nanocomposites also prepared from DMAc solution. The peak of MMT-OH is observed at the same position as C30B,  $2\theta = 4.9^\circ$  ( $d$  spacing = 1.80 nm). For nanocomposites containing MMT-OH, no peaks are observed for either ether-TPU or ester-TPU. This result means that very good dispersion of clay in TPU matrix was achieved both in ether-TPU or ester-TPU/MMT-OH nanocomposites. It is interestingly noted here that good dispersion of clays were obtained for both C30B and MMT-OH nanocomposites even though MMT-OH has only one hydroxyl group in the modifier while C30B has two hydroxyls.

To confirm the XRD results and clearly see the dispersion state of clays in TPU/nanocomposites, TEM pictures were taken. The TEM images of the ether-TPU/clay nanocomposites containing 5 wt % C30B or MMT-OH are shown in Figure 4(a,b), respectively. In these two TEM pictures, very good dispersion of clay platelets close to exfoliation are observed, which is consistent with the earlier XRD results. The TEM images of ester-TPU/clay nanocomposites with 5 wt % C30B or MMT-OH are shown in Figure 5(a,b). Again, good dispersion of clays are observed in both images. But in these



**Figure 3** XRD patterns of ether- and ester-TPU with 5 wt % of (a) C30B and (b) MMT-OH.

ester-TPU nanocomposites, one thing different from the ether-TPU case is that much better dispersion of MMT-OH in Figure 5(b) is observed than C30B in Figure 5(a).

Since one might say that this can be originated from the difference in dispersion of two clays in DMAc, two clays were dispersed in DMAc, and the result was shown in Figure 6. The dispersion was obtained using a magnetic stirrer, and good dispersion was easily obtained within several minutes once magnetic stirring was started. The pictures in the figures were taken 4 h after the stirring was completed. As can be seen from Figure 6, both clays are very well dispersed in DMAc. It means that the difference in the dispersion of MMT-OH and C30B in ester-TPU nanocomposites is due to the difference in affinity between clays and ester-TPUs, where the MMT-OH exhibits better affinity to ester-TPU than C30B. Since ester-TPU has a ester-polyol which has higher hydrophilicity than ether-polyol of ether-TPU, MMT-OH is thought to have higher hydrophilicity than C30B. This actually turns out to be the case since when two clays are dispersed in water, MMT-OH appears to be somewhat dispersible in water while C30B is not as shown in Figure 7. Since MMT-OH has about the same structure as C30B with the slight difference of one hydroxyl attached to longer alkyl chain than C30B, dispersibility of MMT-OH in water indicates that many hydroxyls in MMT-OH are located at the outer surface of clays, by which the hydroxyl group in MMT-OH better contacts water than C30B. This is again consistent

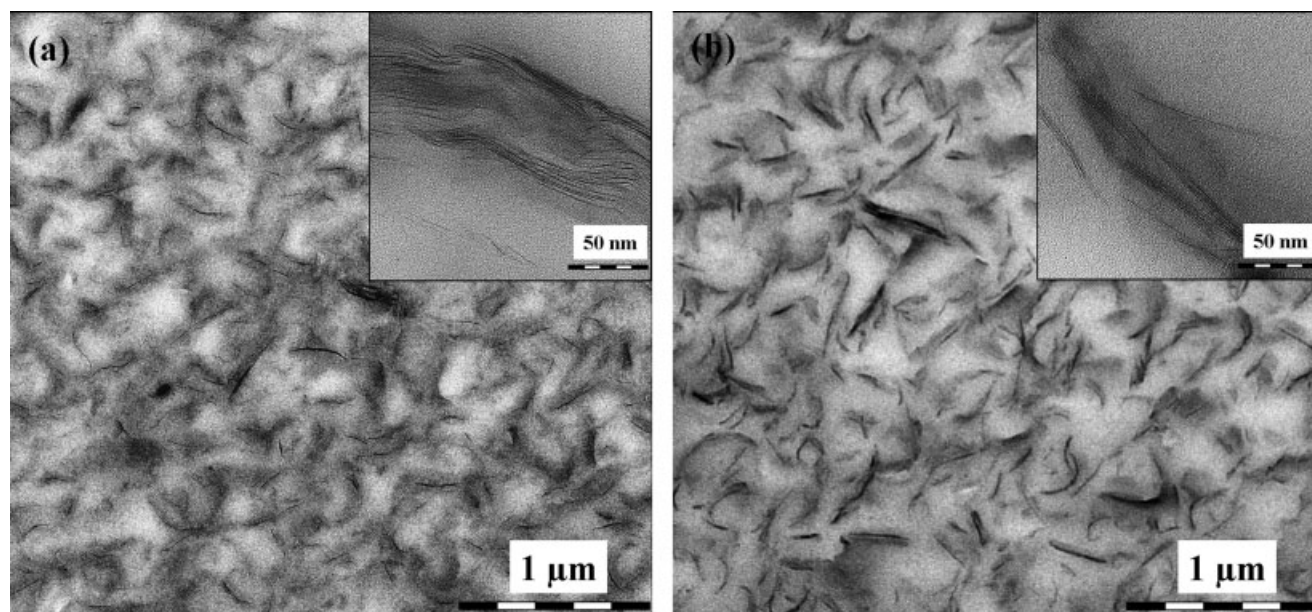


**Figure 4** TEM images of ether-TPU nanocomposites with 5 wt % of (a) C30B and (b) MMT-OH.

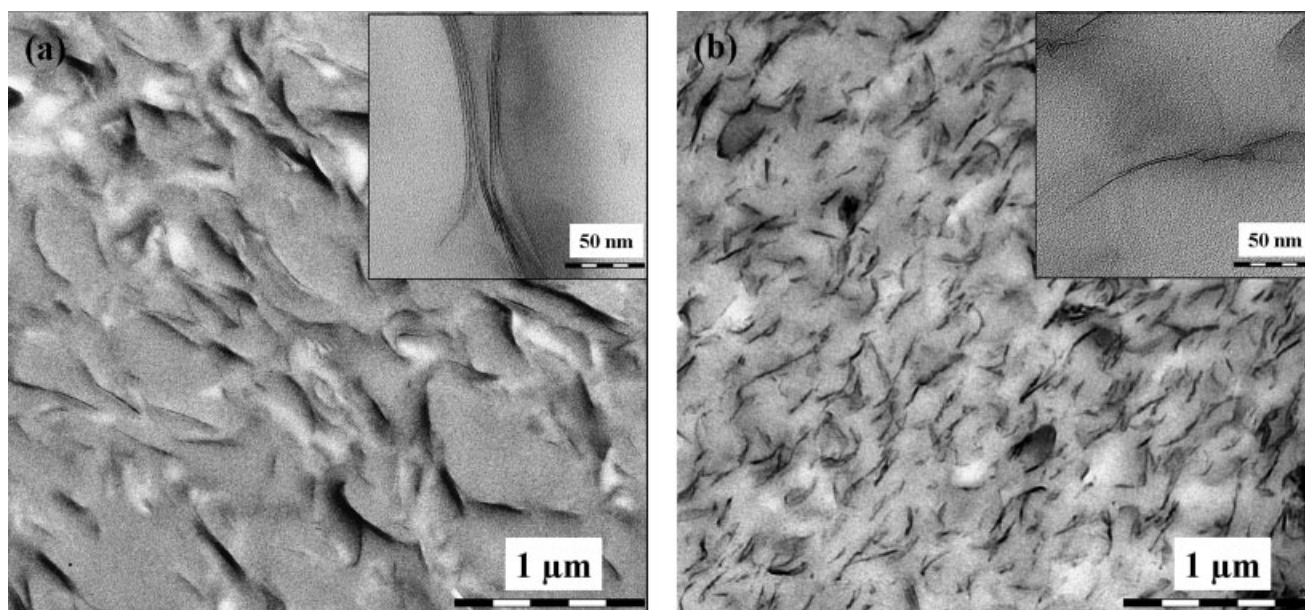


**Figure 5** TEM images of ester-TPU nanocomposites with 5 wt % of (a) C30B and (b) MMT-OH.

with the earlier explanation on the better dispersion of MMT-OH in ester-TPUs.

### Tensile properties

Tensile properties of TPU nanocomposites show similar behavior as the earlier TEM observation. As shown in Figures 8 and 9, the tensile stress at 100 or 200% strain of TPU nanocomposites increased with increasing clay contents in both clays. Two things are noted in these tensile properties results. First, nanocomposites with MMT-OH showed higher increase than C30B ones. Second, ester-TPU nanocomposites showed higher increase than ether-TPU ones. Accordingly, remarkable improvement was

observed for the ester-TPU/MMT-OH nanocomposites and this could be expected from TEM results such as very good dispersion of MMT-OH in Figure 5(b).

For instance, as shown in Table I, about 140% increase compared to neat ester-TPU was observed for tensile stress at 100% strain in ester-TPU/MMT-OH (5 wt %) nanocomposites, while only 25% increase compared to neat ether-TPU was observed in ether-TPU/C30B (5 wt %). Higher values in the tensile properties of MMT-OH nanocomposites can be attributed to the better dispersion of clays than C30B.

These tensile properties result is consistent with TEM and XRD results, where the addition of MMT-OH and C30B led to the nearly exfoliated structure and



**Figure 6** Dispersion state of MMT-OH and C30B in DMAc.

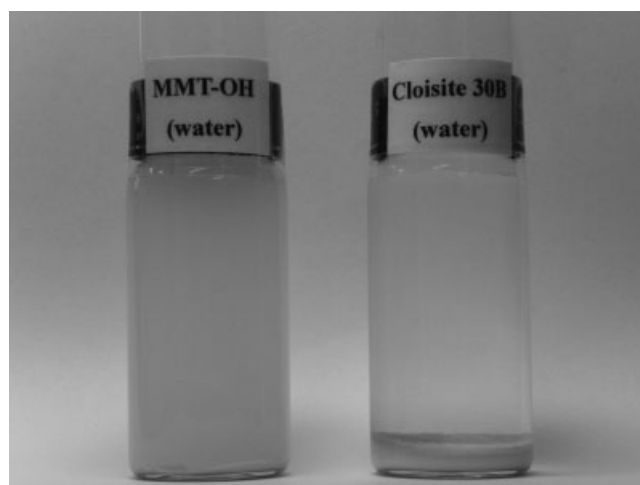


**Figure 7** Dispersion state of MMT-OH and C30B in water.

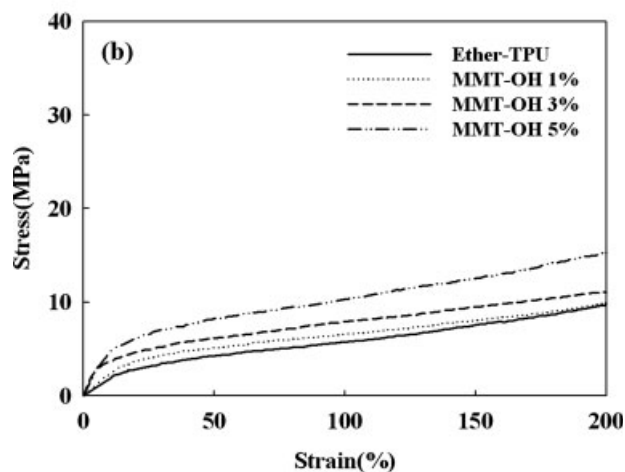
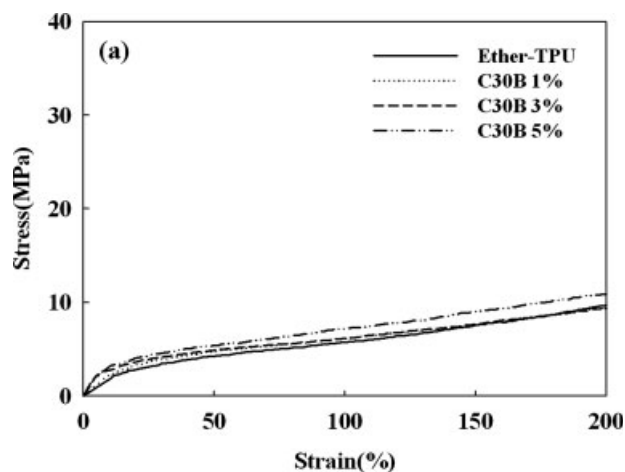


**Figure 8** Tensile stress–strain curves of ether-TPU nanocomposites with (a) C30B and (b) MMT-OH at various clay loadings.

TPU/MMT-OH nanocomposites showed better clay dispersion than TPU/C30B ones.

#### FTIR analysis

To see if the aforementioned clay dispersion and tensile properties improvement is due to the interac-

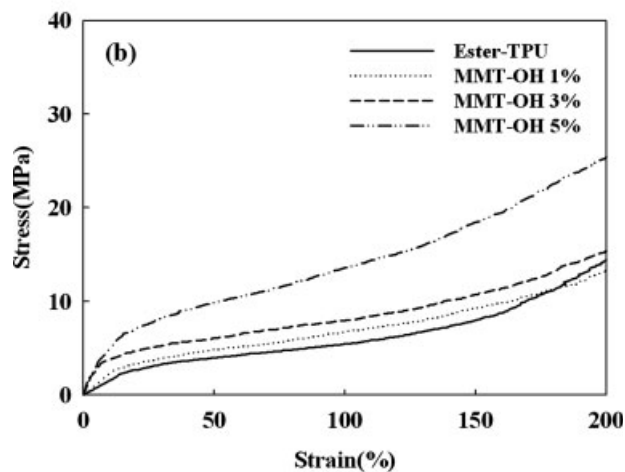
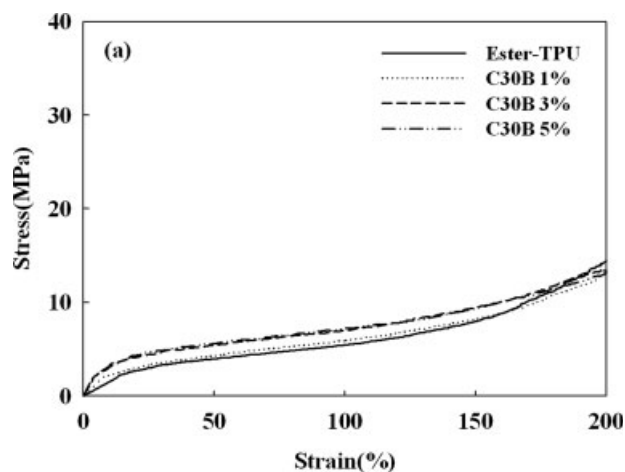


**Figure 9** Tensile stress–strain curves of ester-TPU nanocomposites with (a) C30B and (b) MMT-OH at various clay loadings.

tion between hydroxyls in the clays and TPU matrices, FTIR analyses were carried out. FTIR spectra of ether-TPU and ester-TPU including their nanocomposites with C30B or MMT-OH are shown in Figure 10(a,b), respectively. In ether-TPU shown in Figure 10(a), the  $\text{—NH}$  absorption peak at  $3325\text{ cm}^{-1}$  is due to the hydrogen bonded  $\text{—NH}$  in the urethane

**TABLE I**  
Tensile Properties of TPU Nanocomposites

	Ether-TPU		Ester-TPU	
	Stress at 100% strain (MPa)	Stress at 200% strain (MPa)	Stress at 100% strain (MPa)	Stress at 200% strain (MPa)
TPU	5.6	9.4	5.3	14.4
TPU/C30B				
1 wt %	6.2	9.4	6.8	13.8
3 wt %	6.0	9.0	6.6	12.6
5 wt %	7.0	10.5	7.2	13.2
TPU/MMT-OH				
1 wt %	6.4	9.6	6.8	13.8
3 wt %	7.3	10.1	7.3	14.3
5 wt %	10.1	15.4	12.7	24.2

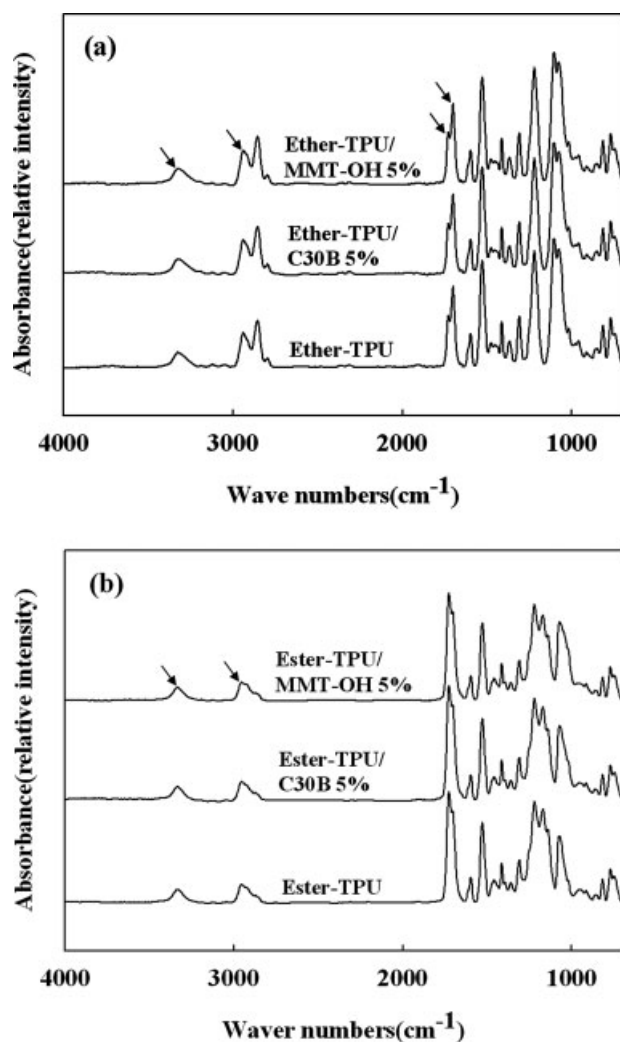


**Figure 10** FTIR spectra of (a) ether-TPU and its nanocomposites with 5% C30B or MMT-OH and (b) ester-TPU and its nanocomposites with 5% C30B or MMT-OH.

linkage. The carbonyl  $\text{—C=O}$  stretchings at  $1730\text{ cm}^{-1}$  and  $1701\text{ cm}^{-1}$  are free and hydrogen bonded ones, respectively. The  $\text{—NH}$  peak of ester-TPU is observed at  $3332\text{ cm}^{-1}$  as shown in Figure 10(b). Since the carbonyl peaks of ester-TPU around  $1700\text{ cm}^{-1}$  are usually irresolvable due to the superposition of peaks from urethanes and ester polyols, it is difficult to distinguish the free and hydrogen bonded carbonyls in ester-TPUs.

Typically the  $\text{—NH}$  groups in the urethane linkage form hydrogen bonds with carbonyls of the urethane linkage in the hard segment in both cases of ether-TPU and ester-TPU. The  $\text{—NH}$  groups are also able to form hydrogen bonding with ether oxygen of ether-polyol in the soft segment in case of ether-TPU and with carbonyls of ester-polyol in the soft segment in case of ester-TPU.

Therefore, examination of  $\text{—NH}$  and carbonyl peaks in the FTIR spectra was performed to get some information on the interaction of clays in the

TPU nanocomposites as done by Pattanayak and Jana.<sup>25–27</sup> The ratio of area under the peaks of  $\text{—NH}$  ( $A_{\text{NH}}$ ) and that of  $\text{—CH}$  ( $2860\text{--}2940\text{ cm}^{-1}$ ) ( $A_{\text{CH}}$ ) was calculated and shown in Table II, where the area under  $\text{—CH}$  stretching was used as the internal standard. Also included in Table II is the ratio of areas under hydrogen bonded carbonyl peaks ( $A_{\text{HCO}}$ ) and free carbonyl peaks ( $A_{\text{FCO}}$ ) for ether-TPU nanocomposites.

In ether-TPU/C30B nanocomposites, the ratio of  $A_{\text{NH}}/A_{\text{CH}}$  (0.26) decreased little and remains about the same as that of neat ether-TPU (0.27) as shown in Table II, while the ratio of hydrogen-bonded carbonyl and free carbonyl ( $A_{\text{HCO}}/A_{\text{FCO}}$ ) increased to 2.67 from 2.58 of neat ether-TPU. This result is similar to the ones of previous studies on ether-TPU/C30B nanocomposites where this kind of change in FTIR analyses were interpreted because of the hydrogen bonding between hydroxyls in the clay and carbonyls of ether-TPU.<sup>18,25</sup>

In ether-TPU/MMT-OH nanocomposites, the ratio of  $A_{\text{NH}}/A_{\text{CH}}$  (0.26) again appeared to be about same as that (0.27) of neat ether-TPU, while  $A_{\text{HCO}}/A_{\text{FCO}}$  value was observed to remarkably increase to 2.88 from 2.58 of pure ether-TPU. This  $A_{\text{HCO}}/A_{\text{FCO}}$  value is also much higher than that (2.67) of TPU/C30B which indicates that more hydrogen bondings were formed in TPU/MMT-OH nanocomposites than TPU/C30B. This means that long hydroxyalkyl chain modifier in MMT-OH is more efficient for hydrogen bonding than short hydroxyalkyl chain in C30B even when MMT-OH has only one hydroxyl group compared to two in C30B.

In ester-TPU/C30B nanocomposites, the ratio of  $A_{\text{NH}}/A_{\text{CH}}$  increased to 0.62 from 0.60 of neat ester-TPU as shown in Table II. This increase may be explained in terms of interaction between  $\text{—NH}$  of urethane segments in the ester-TPU either with C30B or carbonyls of ester-polyols in the ester-TPU as described in the previous studies.<sup>18,25</sup> In ester-TPU/MMT-OH, the ratio of  $A_{\text{NH}}/A_{\text{CH}}$  decreased to 0.58 from 0.60 of the neat ester-TPU. This decrease in  $A_{\text{NH}}/A_{\text{CH}}$  ratio was rather unexpected, since more increase in this ratio than C30B case was

**TABLE II**  
Ratio of the Areas Under the Specific Peaks

	Ether-TPU		Ester-TPU $A_{\text{NH}}/A_{\text{CH}}$
	$A_{\text{NH}}/A_{\text{CH}}$	$A_{\text{HCO}}/A_{\text{FCO}}$	
TPU	0.27	2.58	0.60
TPU/C30B 5%	0.26	2.67	0.62
TPU/MMT-OH 5%	0.26	2.88	0.58

$A_{\text{NH}}$ , area under the hydrogen-bonded  $\text{—NH}$  peak;  $A_{\text{CH}}$ , area under the  $\text{—CH}$  stretching peak;  $A_{\text{HCO}}$ , area under the hydrogen-bonded  $\text{—C=O}$  peak;  $A_{\text{FCO}}$ , area under the free  $\text{—C=O}$  peak.

anticipated if more hydrogen bondings were formed in ester-TPU/MMT-OH. Since TEM image for the ester-TPU/MMT-OH in Figure 5(b) shows a very good and thorough dispersion of MMT-OH in the ester-TPU matrix, MMT-OH clays may reside in both urethane hard segments and ester-polyol soft segments. Accordingly, hydroxyls in MMT-OH may form hydrogen bonding with  $-NH$  in hard segments or carbonyls in soft segments resulting in increase in  $A_{NH}/A_{CH}$  ratio. But at the same time, this MMT-OH dispersion in both segments may interfere the hydrogen bonding between  $-NH$  of urethane segments and carbonyls of ester-polyols as well as interurethane hydrogen bonding in hard segments, which all lead to a decrease in  $A_{NH}/A_{CH}$  ratio. The aforementioned combined result may turn out to be the decrease in  $A_{NH}/A_{CH}$  ratio. FTIR analyses described so far indicate that hydrogen bondings are involved when MMT-OH clays were used to prepare ether- or ester-TPU nanocomposites.

### CONCLUSIONS

Quaternary ammonium salts with a relatively long hydroxyalkyl chain were synthesized by the addition reaction and were used for the organic treatment of montmorillonites. In this modified clay (MMT-OH), hydroxyl groups are observed to be located at the outer surface of clays, which may provide more hydrogen bonding sites compared to the clays having shorter hydroxyalkyl chain modifier (C30B). Both polyester and polyether-based TPU nanocomposites with MMT-OHs showed better tensile properties than the nanocomposites with C30B. Actually, more hydroxyl groups in MMT-OHs are thought to be exposed outside the modified clay, since MMT-OHs were observed to be dispersed in water, while C30B clay was not. Especially, very good clay dispersion was observed in TEM images for ester-TPU/MMT-OH nanocomposites along with the excellent tensile properties. Though direct comparison between MMT-OH nanocomposites and C30B ones cannot be made since MMT-OH has only one hydroxyl group while C30B has two, the earlier results that MMT-OH nanocomposites exhibit better tensile properties than C30B ones having modifiers with two hydroxyls indicate that the position of hydroxyls may be an important factor in determining the properties of TPU/clay nanocomposites. This was thought to be due to the more hydrophilic na-

ture of MMT-OH than C30B observed partly from some water dispersibility of MMT-OH. FTIR analyses show that more hydrogen bondings were observed to form in the nanocomposites with MMT-OH than with C30B.

### References

1. Fornes, T. D.; Hunter, D. L.; Paul, D. R. *Macromolecules* 2004, 37, 1793.
2. Samin, F.; Bourbigot, S.; Jama, C.; Bellayer, S.; Nazare, S.; Hull, R.; Fina, A.; Castrovinci, A.; Camino, G. *Eur Polym J* 2008, 44, 1631.
3. Kelnar, I.; Khunova, V.; Kotek, J.; Kapralkova, L. *Polymer* 2007, 48, 5332.
4. Muralidharan, M. N.; Kumar, S. A.; Thomas, S. J. *Membr Sci* 2008, 315, 147.
5. Calcagno, C. I. W.; Mariani, C. M.; Teixeira, S. R.; Mauler, R. S. *Compos Sci Tech* 2008, 68, 2193.
6. Mittal, V. *Eur Polym J* 2007, 43, 3727.
7. Kojima, Y.; Usuki, A.; Kawasumi, M.; Okada, A.; Fukushima, Y.; Kurauchi, T. *J Mater Res* 1993, 8, 1179.
8. Yoon, P. J.; Fornes, T. D.; Paul, D. R. *Polymer* 2002, 43, 6727.
9. Chiu, F. C.; Lai, S. M.; Chen, Y. L.; Lee, T. H.; *Polymer* 2005, 46, 11600.
10. Hussain, F.; Chen, J.; Hojjati, M. *Mater Sci Eng* 2007, A445-446, 467.
11. Zhao, J.; Morgan, A. B.; Harris, J. D. *Polymer* 2005, 46, 8641.
12. Bharadwaj, R. K.; Mehrabj, A. R.; Hamilton, C.; Trujillo, C.; Murga, M.; Fan, R.; Chavira, A.; Thompson, A. K. *Polymer* 2002, 43, 3699.
13. Yuan, Q.; Misra, R. D. K. *Polymer* 2006, 47, 4421.
14. Zhang, J.; Gupta, R. K.; Wilkie, C. A. *Polymer* 2006, 47, 4537.
15. Lee, M. H.; Dan, C. H.; Kim, J. H.; Cha, J. H.; Kim, S. L.; Hwang, Y. Y.; Lee, C. H. *Polymer* 2006, 47, 4359.
16. Wang, Z.; Pinnavaia, T. *J Chem Mater* 1998, 10, 3769.
17. Jiawen, X.; Zhen, Z.; Hongmei, J.; Sufang, Y.; Xinling, W. *Compos Part A* 2007, 38, 132.
18. Dan, C. H.; Lee, M. H.; Kim, Y. D.; Min, B. H.; Kim, J. H. *Polymer* 2006, 47, 6718.
19. Chavarria, F.; Paul, D. R. *Polymer* 2006, 47, 7760.
20. Solariski, S.; Bernali, S.; Rochery, M.; Devaux, E.; Alexandre, M.; Monteverde, F. *J Appl Polym Sci* 2005, 95, 238.
21. Yao, K. J.; Song, M.; Hourston, D. J.; Luo, D. Z. *Polymer* 2002, 43, 1017.
22. Ma, J.; Zhang, S.; Qi, Z. *J Appl Polym Sci* 2000, 82, 1444.
23. Chang, J. H.; An, Y. U. *J Polym Sci Part B: Polym Phys* 2002, 40, 670.
24. Finnigan, B.; Martin, D.; Halley, P.; Truss, R.; Cambell, K. *Polymer* 2004, 45, 2249.
25. Pattanyak, A.; Jana, S. C. *Polymer* 2005, 46, 3275.
26. Pattanyak, A.; Jana, S. C. *Polymer* 2005, 46, 3394.
27. Pattanyak, A.; Jana, S. C. *Polymer* 2005, 46, 5183.
28. Philip, E. E.; Patrick, G. J.; Kayson, N. *J Am Chem Soc* 1980, 102, 6638.
29. Suhara, T.; Kanemaru, T.; Fukui, H.; Yamagushi, M. *Colloid Surf Physicochem Eng Aspect* 1995, 95, 1.
30. Akerah, A.; Moet, A. *J Mater Sci* 1996, 31, 3589.
31. Alexander, B. M.; Joseph, D. H. *Polymer* 2003, 44, 2313.